Gentian stem harvesting device based on bionic flexible rollers

Hongguang Cui[1], Jinming Zhang[1], Guangshuo Chen[1], Qingchen Tang[1], Wenzhong Huang[2], Liyan Wu[1*]

(1. *College of Engineering, Shenyang Agricultural University, Shenyang 110866, China*;
2. *Fushun Agricultural and Rural Development Service Center, Fushun 113008, China*)

Abstract: Aiming at the problem of incomplete stem removal in the process of *Gentian* root and stem separation, a roller-type *Gentian* stem removal device was designed. Based on the mechanical characteristics of *Gentian* stems and the force analysis of the extraction process, the operating conditions for the complete removal of *Gentian* stems were determined. When the tensile force exerted by the stem-pulling rollers on the *Gentian* stems is less than the tensile force of the *Gentian* stems and greater than the maximum tensile force required for the *Gentian* stems to be removed at the stem bases, the complete removal of *Gentian* stems from the stem base can be realized. The bionic design method is used to construct the bionic flexible surface structure of the stem-pulling rollers by taking the tree frog toe pad as the bionic prototype and investigating its flexible surface microstructure and friction-enhancing characteristics. EDEM simulation software is used to establish the contact model between the bionic flexible stem-pulling rollers and *Gentian* stems, and the optimal structural parameters of the bionic flexible surface are determined through simulation tests. The optimal working parameters of the bionic flexible roller are determined through test rig tests. The experimental results showed that when the diameter of the hexagonal prism of the bionic surface was 5.67 mm, the spacing of adjacent hexagonal prisms was 2.62 mm, and the height of the hexagonal prism was 3.21 mm, the bionic flexible stem-pulling rollers exerted a maximum tensile force of 30.23 N, and the *Gentian* stems were not broken. When the speed of the rollers was 195 r/min, the spacing between stem-pulling rollers was 3.0 mm, and the height of the rollers clamping position was 250 mm, the maximum tensile force required for *Gentian* stem removal was 13.88 N, and the net removal rate reached 94.35%.

Keywords: *Gentian* harvest, bionic design, increased friction, bionic flexible rollers
DOI: 10.25165/j.ijabe.20241706.8453

Citation: Cui H G, Zhang J M, Chen G S, Tang Q C, Huang W Z, Wu L Y. *Gentian* stem harvesting device based on bionic flexible rollers. Int J Agric & Biol Eng, 2024; 17(6): 66–75.

1 Introduction

The Chinese herb *Gentian* is a heat-clearing herb that is the dried roots and rhizomes of *Gentian* striata, *Gentian*, *Gentiana* triflora, or *Gentiana* firma of the *Gentianaceae* family. *Gentian* plants are about 60 cm long, 2.7-3.5 mm in diameter, and slightly thicker at the stem base, with opposite leaves and flush edges. *Gentian* is bitter and cold, and its main uses include anti-inflammatory and anti-dampness, calming abnormal heat in the liver and gallbladder, treating jaundice caused by dampness-heat, swelling and itching of the reproductive system, leucorrhea problems, eczema and itching of the skin, redness and swelling of the eyes due to liver-heat, ringing in the ears and loss of hearing, pain in the ribs and in the mouth, symptoms such as stroke and convulsions, etc.[1-4] The key active ingredient of *Gentian* is *Gentian* Bitter Glycoside. Modern research has shown that *Gentian* has anti-inflammatory and analgesic, hepatoprotective, hypolipidemic, and immune-enhancing effects, and has a high medicinal value. During the harvesting process of *Gentian*, the stems need to be completely removed at the stem base to ensure that no stem breakage occurs, followed by the harvesting of the underground root system, which is still mainly done manually.

Currently, stem removal methods can be categorized into three types: chemical stem removal, cutter stem removal[5], and stem-pulling removal[6-12]. Chemical stem removal refers to the removal of stems using chemicals that cause the stem to die, which is gradually being eliminated for environmental reasons. Cutter stem refers to the removal or churning of the stems by means of components such as knives or discs, and the height of the working parts is usually fixed. Because the height of the stem base of the *Gentian* is not standardized, stubbles are often left after stem removal, which affects the subsequent harvesting and processing of the roots. Stem removal by pulling refers to the use of flexible materials such as belts or pulling rollers to remove stems by applying tensile force through the crop stems. Kou et al.[13] designed a flexible belt-clamping conveyor mechanism, which reduces the breakage rate of onion harvesting and conveying, and realizes stable harvesting. Ge et al.[14] designed a safflower harvesting rollers device, which adopts elastic rubber rollers, to reduce the breakage rate of safflower and improve the quality of harvesting. The use of flexible components for stem lifting and removal not only facilitates the complete removal of the stem at the stem base position but also reduces the

Received date: 2023-07-28 **Accepted date:** 2024-08-17
Biographies: Hongguang Cui, PhD, Associate Professor, research interest: agricultural machinery technology and intelligent equipment, Email: chg7763@syau.edu.cn; **Jinming Zhang**, MS, research interest: agricultural machinery technology and intelligent equipment, Email: zhangjinming0612@163.com; **Guangshuo Chen**, MS, research interest: agricultural machinery technology and intelligent equipment, Email: 18340355282@163.com; **Qingchen Tang**, MS, research interest: agricultural machinery technology and intelligent equipment, Email: 18841553992@163.com; **Wenzhong Huang**, PhD, Professor, research interest: agricultural machinery technology and intelligent equipment, Email: fshwz@126.com.
***Corresponding author: Liyan Wu**, PhD, Professor, research interest: agricultural machinery technology and intelligent equipment. College of Engineering, Shenyang Agricultural University, Shenyang 110866, China. Tel: +86-15942098712, Email: wly78528@syau.edu.cn.

breakage rate of the stem during the removal process.

In recent years, bionic technology has been used widely in the field of agricultural machinery[15-19]. Thirunavukkarasu et al.[20] prepared different shapes of bionic surfaces by observing the microstructure of the skin surface of different animals using 3D printing technology, which effectively improved the coefficient of friction of the working parts. Zhang et al.[21] observed the microstructure of the paws of tree frogs and prepared a micro-nanometer structure on the surface of surgical forceps to improve its friction and reduce the damage to soft tissues. The special ability of tree frogs to move freely between branches without falling stems from the microstructure of their toe pads, in which the arrangement of hexagonal prisms provides superior grip and stability. When the toe pad is subjected to a load, the deformation of the toe pad bridges the grooves. This allows the toe pad to form a monolithic continuous surface that more easily replicates the shape of the contact surface, thereby increasing the contact area for improved friction and adhesion. The application of bionic surface technology to working parts can significantly improve their working performance. The use of bionic technology on the stem-pulling rollers can effectively improve their friction performance and reduce the damage to the stems, thus effectively completing the removal of the *Gentian* stems and realizing the net-removal effect.

Aiming at the problem of existing *Gentian* stem-pulling devices leaving broken stems, which leads to stem residues affecting the harvesting and subsequent processing of the medicinal roots, this study designs a *Gentian* stem-pulling device based on bionic flexible stem-pulling rollers and analyzes the principles of the working conditions in which the *Gentian* stems are completely removed. The test is based on the microstructure of the toe pad of the lord's tree frog as a bionic prototype, which consists of many hexagonal prismatic units at the toe end. A bionic surface was designed and prepared to be fixed on the rollers. A prototype was made and tested to determine the optimum operating parameters, which are intended to provide a design reference for *Gentian* stem-pulling machinery.

2 Design of bionic flexible roller

2.1 Basic characteristics of *Gentian*

The biological structure of *Gentian* is shown in Figure 1. It consists of the aboveground stem, the intermediate union (called the "stem base"), and the underground root system (the medicinal part).

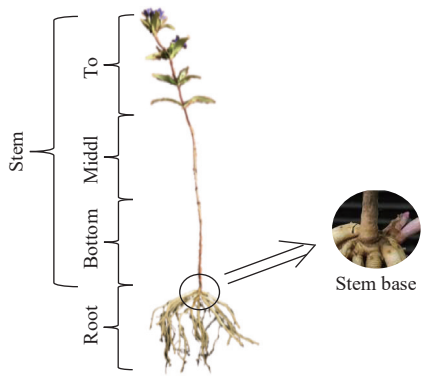

Figure 1 The complete structure of the *Gentian*

Fifty intact *Gentian* plants with stems were selected as experimental material according to the different positions of the stems (bottom, middle, and top). The length of the *Gentian* stems and the diameter of each part were measured using digital vernier callipers (accuracy 0.01). Tensile tests were carried out with the help of the Instron 5944 universal testing machine to determine the tensile strength of the various parts of the *Gentian* stems as well as the tensile strength at the stem base. The detailed data are listed in Table 1.

Table 1 Statistical results of *Gentian* physical properties

Statistical parameters	Overall length/mm	Diameter/mm			Compressive strength/N			
		Bottom	Middle	Top	Bottom	Middle	Top	Stem base
Maximum value	541.00	3.44	3.76	2.98	173.92	195.55	60.69	35.08
Minimum value	315.00	3.00	3.16	2.26	113.14	140.63	36.84	11.37
Average value	398.77	3.16	3.34	2.64	142.00	172.86	48.90	23.62
Standard deviation	65.78	0.18	0.24	0.33	22.27	21.22	10.69	6.28
Coefficient of variation/%	6	6	7	12	16	12	22	27

2.2 Analysis of the mechanism for *Gentian* stem removal

As a key component of the *Gentian* stem-pulling structure, the radius and rotational speed of the bionic flexible stem-pulling rollers have an important impact on the quality of work. To determine the radius and rotational speed of the bionic flexible stem-pulling rollers, mechanical analysis of the *Gentian* stem-pulling process was carried out, and the results are shown in Figure 2.

$$(F_{f1}+F_{f2})\cos\alpha > (F_1+F_2)\sin\alpha + F_b \tag{1}$$

$$\mu > \tan\alpha + \frac{F_b}{(F_1+F_2)\cos\alpha} \tag{2}$$

where, α is the initial stem feed angle, (°); μ is the coefficient of friction between rollers and stem; F_1 is the pressure of rollers on stems, N; F_2 is the pressure of rollers on stems, N; F_{f1} is the friction of stem-pulling rollers on stems, N; F_{f2} is the friction of stem-pulling rollers on stems, N; and F_b is the tensile strength at stem base position, N.

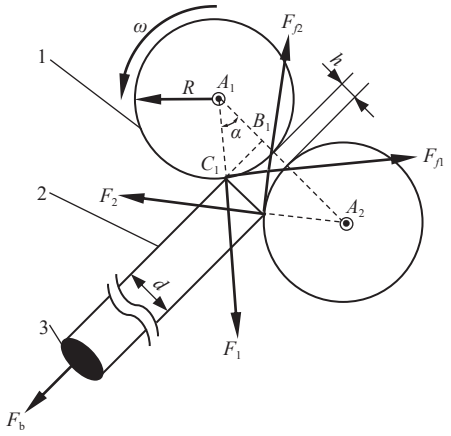

1. Stem-pulling roller 2. Stem 3. Stem base

Figure 2 Analysis of the *Gentian* stem removal process

As shown in Equation (1), reducing the initial feeding angle and increasing the friction coefficient between the rollers and the stems is more conducive to the removal of the *Gentian* stems. Selecting the largest possible roller radius within a reasonable range and minimizing the feeding angle is recommended. A bionic surface modeled off of tree frog toe pads was made on the surface of rollers with good flexibility, which allows for a better fit between the rollers and the *Gentian* stems contact surface. A bionic surface with a high degree of flexibility can transfer a portion of the deformation of the *Gentian* stem to the bionic surface of the rollers, thus

providing a degree of protection against breakage. In $\Delta A_1B_1C_1$:

$$\cos\alpha = \frac{A_1B_1}{A_1C_1} = \frac{\frac{2R+h-d}{2}}{R} = 1+\frac{h-d}{2R} \quad (3)$$

Transformed to:

$$R \geq (d-h)\left[2\left(1-\frac{1}{\sqrt{1+\mu^2}}\right)\right]^{-1} \quad (4)$$

where, R is the stem-pulling roller radius, mm; h is the rollers spacing, mm; d is the diameter of the stem, mm; C_1 is the initial contact point of the rollers with the stem; and B_1 is the vertical projection of C_1 on the axis line of the rollers.

According to the pre-experimental results, it is known that the diameter of the *Gentian* stem is 2.64-3.16 mm. In the *Gentian* stem compression test, the average compression displacement was 1.03 mm when the *Gentian* stem was crushed. To ensure that the stem is not broken and has a certain pressure, take the stem-pulling rollers' spacing as 2.8 mm. The coefficient of friction between the *Gentian* stem and the 3D printing material is 0.6-1.1, which is brought into Equation (4) to find the radius of the bionic flexible stem-pulling roller as R≥55 mm. Considering that the increase of the radius of the bionic flexible stem-pulling rollers will enhance the removal ability, the radius of each bionic flexible stem-pulling roller is R=70 mm.

The circumferential linear velocity v of the bionic flexible stem-pulling roller is:

$$v = \omega R = \frac{2\pi nR}{60} \quad (5)$$

where, ω is the angular velocity of rollers, rad/s; n is the rotating speed of rollers, r/min; and v is the circumferential linear velocity of the roller, m/s.

According to the Handbook of Agricultural Machinery, the ratio of the circumferential linear speed of the bionic flexible stem-pulling rollers to the forward speed of the machine is taken to be 2:3. According to the harvest requirements and the results of the pre-test, the forward speed of the *Gentian* stem removal machine is 0.5-1.0 m/s. Substituting into Equation (5), we find that the rotational speed of each bionic flexible stem-pulling roller is 144-239 r/min.

2.3 Analysis of the mechanism of increased friction on bionic surfaces

Zhang et al.[21] elaborated on the strong adsorption and friction properties of the toe pads of tree frogs. In this study, a live lord's tree frog (*Litoria caerulea*) was used as a biological sample, and its toe pad parts were cut with a sharp surgical blade. Firstly, the toe pad samples were washed with 0.1 mol/L phosphate buffer and fixed by immersion in a 2.5% glutaraldehyde solution for 24 h. Subsequently, the samples were dehydrated in a series of concentration gradients of alcohol, immersed in tert-butanol, and vacuum dried at 0°C. The samples were treated with a metal coating. Observations were made by scanning electron microscopy (SEM). The observation results are shown in Figure 3.

Through the observation of SEM, it was found that the surface of the toe pads of tree frogs is covered with densely arranged columnar epithelial cells, which mostly present a hexagonal shape. The structure of the tree frog toe pads is shown in Figure 3b. The epithelial cells on the surface of the toe pads consist of a large number of flat-surfaced, neatly arranged hexagonal units, which are separated by grooves of different lengths and directions for mucus storage. The diameters of the inner circle of hexagons are both about 1 μm, while the widths of the grooves are about 10 μm and the depths are about 10 μm.

Figure 3c presents an enlarged photograph of several hexagonal units. It can be vaguely observed in the figure that the surface of each hexagonal cell consists of numerous smaller hexagonal cells, which are separated by smaller grooves (as shown in Figure 3d). The diameters of the small units are about 0.1 to 0.4 μm, while the widths of the small grooves are about 40 nm and the depths are about 0.2 μm.

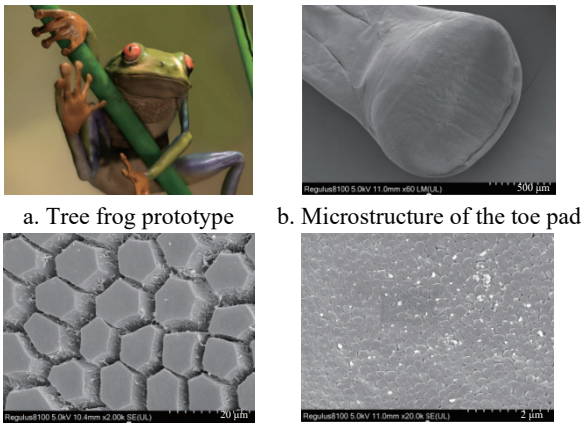

a. Tree frog prototype b. Microstructure of the toe pad

c. Toe pad level 1 structure d. Toe pad level 2 structure

Figure 3 Microstructure of the tree frog's toe pad

When pressure is applied to the tree frog's feet, the toe pads deform, causing the grooves to close, resulting in a tight fit that contacts the material surface. This groove closure significantly increases the contact area, which improves the friction performance of the pad. Tree frogs have flexible toe pads, and when they come into contact with objects, the deformation of those objects can be replicated on the soft surface of the toe pads, thus protecting the object being contacted to a certain extent. The grooves between the hexagonal prisms drain fluids away, thus reducing friction of boundary and fluid. Applying the properties of the tree frog toe pads to the rollers used to pull out the stem improves the friction of the rollers against the *Gentian* stems and reduces the risk of stem breakage during the working process[22,23].

2.4 Design of bionic flexible surfaces

Combining the SEM observations and literature research results, and considering the structure and size of the actual stem-pulling rollers, this design integrates the microstructural features of the tree frog toe pads from the perspective of bionics by applying the principle of similarity engineering to design and develop a bionic surface. Considering the diversity of tree frog toe pad structures, by comparing bionic surfaces with different geometrical shapes such as triangular, rhombic, and square, it has been pointed out that the hexagonal prism shape had the best lateral and longitudinal friction[21]. Therefore, hexagonal prisms were chosen as the basic unit of the bionic flexible surface of the stem-pulling rollers. The staggered arrangement is used to design the bionic surface. The key geometric parameters for the design of the bionic surface include the height and diameter of the hexagonal prisms and the spacing of adjacent hexagonal prisms. The design was realized by applying rubber sleeves with bionic flexible surfaces to the stem-pulling rollers for easy replacement and maintenance. This is shown in Figure 4.

The Bionic Flexible Sleeve was fabricated using 3D printing technology. The material chosen was TPE-83A, a thermoplastic elastomer with high strength and toughness. TPE-83A has a printing temperature range of 220°C-230°C, a density of 1.14 g/cm^3, a

tensile strength of 32 MPa, an elongation at break of 420%, and a hardness rating of 83A, which make it an ideal choice for the fabrication of the bionic flexible stem-pulling rollers rubber sleeve. The 3D printer selected is model CT-228, manufactured by Shenzhen Creative 3D Technology Co. The printer has a highly accurate control capability, with a maximum nozzle operating temperature of 250°C, a positioning accuracy of 0.012 mm, and a printing accuracy within the range of ±0.1 mm, which ensures that the printed rubber sleeve has a high degree of precision and good surface quality.

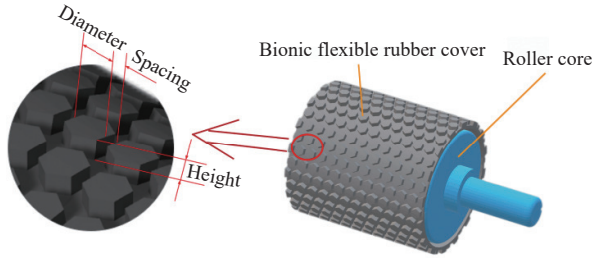

Figure 4 Structural parameters of bionic flexible rollers

The established 3D model of the bionic flexible stem-pulling rollers was converted to STL format and imported into Ultimaker CURA 6.0 slicing software. The slicing parameters for 3D printing are listed in Table 2.

Table 2 Parameters of the 3D printed slices

Performance/parameters	Numerical values
Story height/mm	0.2
Wall thickness/mm	1.35
The thickness of the top and bottom floors/mm	0.8
Filling density/%	15.0
Print temperature/°C	235.0
Flow rate/%	120.0
Print speed/(mm·s^{-1})	30.0
Platform attachment type	Raft
Cooling	off

3 Discrete model for *Gentian* stem and bionic flexible stem-pulling roller

3.1 Determination of mechanical parameters of the *Gentian* stem

To construct a simulation model of *Gentian* stems with bionic flexible rollers, the intrinsic parameters of *Gentian* stems were determined. A halogen water content tester was chosen to measure the water content of *Gentian* stems, and the average water content of *Gentian* stems was 43%. The specific gravity bottle method was used to measure the volume of *Gentian* stems, and an electronic balance with an accuracy of 0.001 g was used to measure the mass of *Gentian* stems. The density of *Gentian* stems was calculated to be 850 kg/m^3 by averaging several measurements.

The compression and tensile tests were carried out on *Gentian* stems by the Instron universal testing machine. The pressure was applied in the axial direction at a rate of 10 mm/min until the stems broke. The transverse and longitudinal strains of the *Gentian* stems were obtained by measuring with an extensometer. The Poisson's ratio of the *Gentian* stems was calculated from Equation (5). The elastic modulus of *Gentian* stems was measured to be18.17 MPa by stretching the stems at a speed of 40 mm/min, and the shear modulus of *Gentian* stems was found to be 2.38 MPa by Equation (6). The model parameters are listed in Table 3.

$$\varepsilon = \frac{|e'|}{|e|} = \frac{W_1 - W_2}{L_1 - L_2} \tag{6}$$

$$G = \frac{E}{2(1+\varepsilon)} \tag{7}$$

where, ε is the Poisson's ratio of the *Gentian* stem; e' is the transverse deformation of the *Gentian* stem, mm; e is the longitudinal deformation of the *Gentian* stem, mm; W_1 is the longitudinal diameter of the *Gentian* stem before compression, mm; W_2 is the longitudinal diameter of the *Gentian* stem after compression, mm; L_1 is the lateral diameter of the *Gentian* stem before compression, mm; L_2 is the lateral diameter of the *Gentian* stem after compression, mm; G is the *Gentian* stem shear modulus, MPa; and E is Young's modulus of the *Gentian* stem, MPa.

Table 3 Mechanical parameters of the simulation model

Characteristic parameters	*Gentian* stem	TPE-83A
Poisson's ratio	2.81	0.4
Shear modulus/MPa	2.38	32
Density/(kg·m^{-3})	850	1140

Measurement of the dynamic and static coefficients of friction between the *Gentian* stem and TPE-83A was made using a homemade friction meter. The dynamic and static friction factors between the *Gentian* stem and TPE-83A were calculated using Equation (7) and are listed in Table 4.

$$\mu = \tan\theta \tag{8}$$

where, μ is the *Gentian* stem-TPE-83 static coefficient of friction; and θ is the angle with the horizontal plane when the support plate stops lifting, (°).

Table 4 *Gentian* stem - TEP-83A contact parameters

Characteristic parameters	*Gentian* stem - TEP-83A
Recovery factors	0.4
Dynamic friction factor	0.87
Static friction factor	1.14

A free fall test was used to determine the recovery coefficient of the *Gentian* stem[24], which was calculated from Equation (8) and is listed in Table 4.

$$f = \sqrt{\frac{\Delta h}{h}} \tag{9}$$

where, f is the recovery factor for the *Gentian* stem; h is the fall height of the *Gentian* stem, mm; and Δh is the height of the *Gentian* stem pop-up, mm.

3.2 Simulation contacts model selection and model construction

The *Gentian* plant was modeled using Solidworks 2020 software based on the above-measured geometric parameters of the *Gentian* stem. The *Gentian* stem was simplified to a cylinder with a length of 400 mm and a diameter of 3.31 mm and attached to the root. The established 3D model of the *Gentian* stem was converted into an STL format file. To provide a contour base for particle filling in EDEM[25]. The Hertz-Mindlin model was used to build the particle model as shown in Figure 5a.

A multisphere particle filling method was used to construct a discrete meta-model of a *Gentian* stem. A particle factory was established to fill particles into the 3D model of the *Gentian* stem by dynamic generation. The generation rate of the particle factory

was 0.5 kg/s, and the generation time was 3.5 s until the model was filled, as shown in Figure 5b. Using the Hertz-Mindlin model[26] to build the particle model as a whole, it is invalid to carry out the numerical calculation of the fracture process, so it cannot be used for the simulation of the tensile process of the *Gentian* stem simulation. Based on the Hertz-Mindlin model, the inter-particle bonding effect was added. The Hertz-Mindlin with bonding model was used to bond the individual *Gentian* stem particle unit models, and when the maximum normal stress and maximum tangential stress between particles exceeded the predefined critical values, the bonding bond breaks. The parameters of the bond model were set according to the above-measured mechanical properties of the *Gentian* stems, as shown in Figure 5c[27].

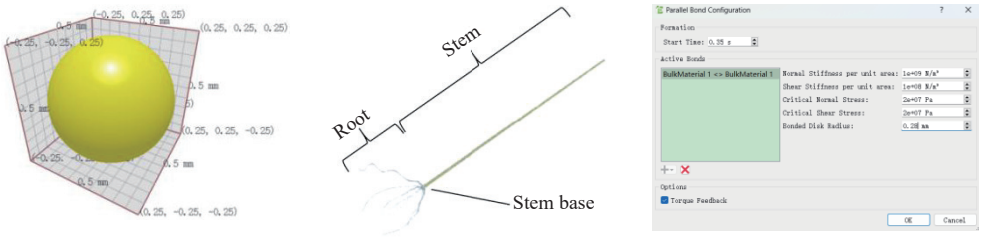

a. Gentian stem particle unit b. Gentian stem model c. Setting parameters for the bond model

Figure 5 Discrete element model and parameters for *Gentian* stem

The simplified model of the bionic flexible stem-pulling rollers was converted to STL format and imported into EDEM. In the simulation setup, the negative direction of the *Y*-axis was defined as the direction of downward gravitational acceleration, and its value was set to 9.81 m/s². The distance between the two rollers was set to 3 mm, and their axial rotational speed was adjusted to 191 r/min and rotated in phase. The simulation model is shown in Figure 6.

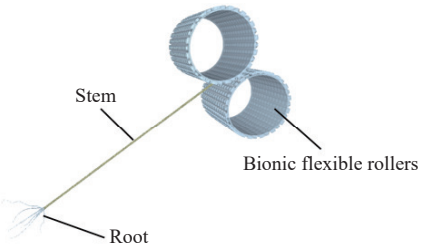

Figure 6 Simulation model

3.3 Simulation Results and Analysis

In the simulation analysis of the *Gentian* stem handling process, a key observation point is the stress response process at the contact position between the *Gentian* stem and the bionic flexible stem-pulling rollers. As shown in Figure 7, when the *Gentian* stem was fed between the bionic flexible stem-pulling rollers, it was first subjected to friction and pressure between the bionic flexible stem-pulling rollers. This action caused the bonding force between *Gentian* stem particle units to be affected, which in turn led to localized fracture phenomena. As the bionic flexible stem-pulling rollers continued to rotate, these localized fracture areas gradually moved to the outside of the rollers, but no complete fracture was observed.

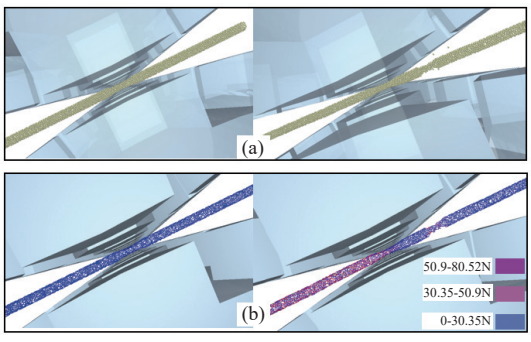

Figure 7 Stem tensile process at the clamping position of the roller

The stretching process experienced by the *Gentian* stem under the tension of the bionic flexible stem-pulling roller is also one of the focuses of this study. As shown in Figure 8, the tensile force at the stem base position of the *Gentian* stem was generated by the frictional force at the contact point between the bionic flexible stem-pulling rollers and the *Gentian* stem, resulting in the contraction of the *Gentian* stem. As the tensile force continued to increase, the bond between the particle units began to break gradually. When this tensile force exceeded the maximum tensile strength at the base of the stem, the bond between the stem and the granular unit eventually broke completely, signaling the removal of the stem.

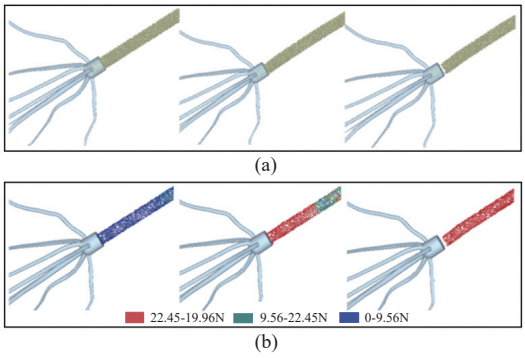

Figure 8 Stem tension process at the stem base

3.4 Experimental design and results

Based on the observation and theoretical analysis, the diameter of the hexagonal prism X_1, the spacing of adjacent hexagonal prisms X_2, and the height of the hexagonal prism X_3 were selected as the experimental factors. The Box-Behnken experimental design was used. With tensile force on *Gentian* stems Y_1 and pressure on *Gentian* stem Y_2 as indicators of bionic surface structural parameters, experimental factors and levels are listed in Table 5.

Table 5 Coding table of experimental factors and levels

Factor level	Hexagonal prism diameter X_1/mm	Spacing of adjacent hexagonal prisms X_2/mm	Hexagonal prism height X_3/mm
–1	4	2	2
0	5	3	3
1	6	4	4

In Design-Expert, according to the Box-Behnken Design (BBD) test scheme, the test results are listed in Table 6. Through

the analysis, the regression model equations of tensile force on *Gentian* stems Y_1 and pressure on *Gentian* stem Y_2 were fitted out respectively to explore the impact of various factors on the evaluation indicators and the interaction law.

Table 6 Results and design of tests

No.	X_1	X_2	X_3	Y_1	Y_2
1	0	1	1	34.28	97.12
2	1	1	0	34.12	86.32
3	–1	0	–1	11.32	67.41
4	0	0	0	32.23	75.32
5	1	0	–1	11.68	75.25
6	0	0	0	28.23	80.31
7	1	0	1	30.23	84.35
8	0	0	0	22.89	84.43
9	0	0	0	30.32	80.12
10	–1	1	0	34.23	92.43
11	0	1	–1	18.18	74.35
12	1	–1	0	24.5	77.94
13	0	0	0	27.98	81.98
14	0	–1	1	13.23	72.85
15	–1	–1	0	11.32	69.46
16	–1	0	1	15.83	90.16
17	0	–1	–1	11.23	68.84

3.5 Experiment results and analysis

As shown in Table 7, through the regression analysis of the test results, it can be seen that the significant factors affecting Y_1 in descending order are X_2, X_3, and X_1, while the significant factors affecting Y_2 in descending order are X_3, X_2, and X_1. This is because the spacing between hexagonal prisms and the height of the hexagonal prism changes in the process of removal, producing a furrow force and thereby increasing the removal force exerted by the pulling-stem rollers on *Gentian* stems. If the spacing is too large, it will reduce the actual contact area, which will reduce the friction and the removal forces. The height of the hexagonal prism and the spacing between hexagonal prisms had a very significant effect on the pressure on *Gentian* stems, while the diameter of the hexagonal prism had no significant effect on the pressure on the *Gentian* stems. Higher spacing of the hexagonal prism and height of the hexagonal prism may cause a concentration of stress, which may result in more pressure on the *Gentian* stems.

Table 7 Analysis of test results

Source	Sum of squares	*df*	Mean square	*F*-value	*p*-value
Model	1277.15/1110.97	9	141.91/123.44	18.1/17.94	0.0005**/0.0005*
X_1	96.81/2.42	1	96.81/2.42	12.35/0.35	0.0098**/0.5718
X_2	457.99/467.11	1	457.99/467.11	58.4/67.89	0.0001**/0.0001**
X_3	211.77/429.68	1	211.77/429.68	27/62.54	0.0013**/0.0001**
X_1X_2	44.16/53.22	1	44.16/53.22	5.63/7.73	0.0494*/0.0273*
X_1X_3	49.28/46.58	1	49.28/46.58	6.28/6.77	0.0406*/0.0353*
X_2X_3	49.70/87.98	1	49.7/87.98	6.34/12.79	0.0400*/0.0090**
X_1^2	19.04/4.68	1	19.04/4.68	2.43/0.68	0.1632/0.4368
X_2^2	0.11/0.011	1	0.11/0.011	0.014/0.002	0.9093/0.9690
X_3^2	336.43/20.26	1	336.43/20.26	42.9/2.94	0.0003**/0.1299
Residual	54.89/48.16	7	7.84/6.88		
Lack of Fit	6/3.54	2	2/1.18	0.16/0.11	0.9156/0.9525
Pure Error	48.9/44.63	5	12.22/11.16		
Cor Total	1332.05/1159.14	16			

Combined with the analysis above, to optimize the performance of bionic flexible surfaces, it is necessary to maximize the tensile force on the *Gentian* stem and minimize the pressure on the *Gentian* stem. To seek the optimal parameter combination, it is necessary to conduct parameter optimization on multiple targets. Design-Expert was used to optimize and solve each parameter. The optimal solutions are: diameter of hexagonal prism 5.67 mm, spacing of adjacent hexagonal prisms 2.62 mm, height of hexagonal prism 3.21 mm, tensile force on *Gentian* stems 28.58 N, pressure on *Gentian* stem 79.91 N. The test was carried out in the bionic flexible stem-pulling rollers test rig, with the rotational speed at 191 r/min and the spacing of the stem-pulling rollers at 2.8 mm. The *Gentian* stem pulling test was carried out 10 times. The average value of the tensile force applied to the *Gentian* stems was measured as 30.23 N, and the *Gentian* stems were not broken. The test results were similar to the predicted values.

4 Performance testing of bionic flexible stem-removal rollers test rig

4.1 Test conditions and methods

The experiment was conducted in March 2023 at Qingyuan Manchu Autonomous County, Fushun City, Liaoning Province, China, and the materials used in the research experiment were healthy *Gentian* plants with a sterile and disease-free growth cycle of 3 years. As shown in Figure 9, the bionic flexible stem-pulling rollers test rig consists of a frame, an upper computer, two-speed motor controllers, a stable voltage supply, two AC speed-regulated motors, a data acquisition card, a pair of bionic flexible stem-pulling rollers, a tension sensor lifting ring, and a tension sensor.

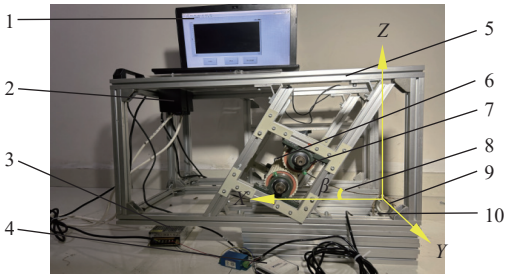

1. Upper computer 2. Speed motor controller 3. Stable voltage supply 4. Data acquisition card 5. Frame 6. AC speed-regulated motors 7. bionic flexible stem-pulling rollers 8. *Gentian* stem 9. Tension sensor lifting ring 10. Tension sensor

Figure 9 Bionic flexible stem-pulling rollers test rig

The overall size parameter of the bionic flexible stem-pulling roll test rig frame is 780 mm×380 mm×370 mm, which is assembled by 30 mm×30 mm square aluminum profiles. The tensile sensor is used to measure the data of tensile force on the material and output as a voltage signal. The range of the tension sensor is 0-20 kN, and the accuracy is 0.03%. The voltage signal collected by the tension sensor is uploaded to the host computer through the NI-6009 data acquisition card. The upper computer consists of a laptop computer and self-compiled Labview software. The upper computer converts the voltage signal collected by the tension sensor to the tension value through the linear regression equation obtained according to the calibration through the compiled tension detection software, which is displayed and saved through the front panel.

The bionic flexible stem-pulling rollers are directly driven by two AC speed control motors, and the speed of the bionic flexible stem-pulling rollers is adjusted by the speed motor controller, with a speed range from 0 to 300 r/min. The bionic flexible stem-pulling rollers are installed on four movable cross beams. The spacing

between stem-pulling rollers and the height of the clamping position can be adjusted by moving the crossbar. The working principle of the bionic flexible stem-pulling rollers test bench is as follows: a pair of bionic flexible stem-pulling rollers are driven by an AC speed motor to rotate in opposite directions, and the *Gentian* stems are affected by the tension generated by the rollers until they are broken or pulled out from the stem bases. The speed of the rollers is adjusted using two-speed motor controllers. The maximum tensile force exerted on the *Gentian* stem breakage is recorded by the tension sensor, and the position of the *Gentian* stem breakage is recorded. A three-dimensional coordinate system is established with the position of the apex of the tension sensor lifting ring of the tension sensor as the origin. Consider the *X*-*Y* plane as the actual working ground surface. The low surface of the frame coincides with the *X*-*Y* plane. The plane where the axes of the pair of rolls are located is at 60° to the *X*-*Y* plane. The root of the *Gentian* is fixed to the tension sensor lifting ring of the tension sensor through the rolling belt, the base of the *Gentian* stem coincides with the origin, and the *Gentian* stem extends upward along the *Z*-axis, as shown in Figure 9.

4.2 Test factors and index selection

Based on the observation and theoretical analysis of the pre-test, it can be seen that the speed and spacing of the rollers have an important effect on the removal of *Gentian* stems. When the *Gentian* stems are removed along different directions, there are differences in the process of *Gentian* stem fracture and in the tension force on the *Gentian* stems, which in turn lead to differences in the required magnitude of the tension force for *Gentian* stem removal.

The effects of rollers speed (X_1), spacing between stem-pulling rollers (X_2), and height of rollers clamping position (X_3) on the maximum tensile force required for *Gentian* stem removal (Y_1) and the net removal rate (Y_2) were explored. The Box-Behnken Design method combined with the response surface method were used to conduct experiments and explore the interaction effects of influence factors on indicators. A regression model of influence factors and evaluation indicators was established through analysis of variance. The test factors and levels are listed in Table 8.

Table 8 Coding table of experimental factors and levels

Factor level	Rollers speed X_1/(r·min^{-1})	Spacing between stem-pulling rollers X_2/mm	Clamping position height X_3/mm
–1	144	2	180
0	191.5	2.75	241.5
1	239	3.5	303

For this test, we referred to GB/T 8097-2008 Test Methods for Harvesting Machinery-Combine Harvester. Before the test, the machine was adjusted to the working position, and the test was conducted after the machine was adjusted and stabilized. Well-grown and disease-free *Gentian* stems were selected for the test, and the length, diameter, and other basic parameters of the stems were measured before the test. Completing stem removal with a smaller removal force can reduce energy consumption, and a high net removal rate can improve quality work. The maximum removal force and net removal rate were selected as the test indices. Due to the variation of the clamping position height of rollers, the *Gentian* stems form an angle with the *X*-*Y* plane β. The maximum tensile force required for *Gentian* stem removal measured by the transducer is recorded as T_s. Therefore, the actual maximum tensile force required for *Gentian* stem removal Y_1 applied to the *Gentian* stem is shown in Equation (9). Net removal is defined as the breakage of the *Gentian* stems from the stem base under the tensile force exerted by the stem-removal rollers, leaving only the intact root of the herb without stubble. The net removal rate is calculated by recording the total number of samples as N, the number of stem breaks at the stem base as N_1, and the net removal rate Y_2 as an evaluation index, as shown in Equation (10).

$$Y_1 = T_s \sin\beta \tag{10}$$

$$Y_2 = \frac{N_1}{N} \times 100\% \tag{11}$$

The test results were analyzed by ternary quadratic regression using Design-Expert software. Quadratic polynomial response surface regression models were established for the maximum tension and net removal rate of *Gentian* roller speed, spacing between stem-pulling rollers, and clamping position height of the roller, and the regression models were analyzed by ANOVA. The results and design of the tests are listed in Table 9.

Table 9 Results and design of tests

No.	X_1	X_2	X_3	Maximum tensile force Y_1/N	Net removal rate Y_2/%
1	0	1	–1	24.19	91.16
2	0	0	0	11.56	98.28
3	–1	1	0	24.26	90.78
4	1	0	1	24.96	89.45
5	1	–1	0	23.03	85.45
6	0	0	0	14.06	98.19
7	–1	–1	0	29.29	86.22
8	–1	0	–1	34.23	87.55
9	0	0	0	12.63	98.37
10	0	1	1	21.77	95.79
11	1	0	–1	23.96	86.36
12	0	0	0	12.21	96.78
13	1	1	0	23.99	95.19
14	0	–1	1	19.39	86.92
15	0	0	0	13.67	98.32
16	0	–1	–1	30.23	86.58
17	–1	0	1	22.37	85.98

4.3 Test results and parameter optimization

The significance of the regression coefficients was tested for Y_1. The analysis results are listed in Table 10.

Table 10 Regression equation analysis of variance results

Source	Sum of squares	*df*	Mean square	*F*-value	*p*-value
Model	720.93	9	80.1	108.62	< 0.0001**
X_1	25.24	1	25.24	34.23	0.0006**
X_2	7.47	1	7.47	10.13	0.0154*
X_3	72.72	1	72.72	98.61	< 0.0001**
X_1X_2	8.97	1	8.97	12.16	0.0102*
X_1X_3	41.34	1	41.34	56.07	0.0001**
X_2X_3	17.72	1	17.72	24.03	0.0017**
X_1^2	230.62	1	230.62	312.73	< 0.0001**
X_2^2	101.75	1	101.75	137.97	< 0.0001**
X_3^2	159.42	1	159.42	216.18	< 0.0001**
Residual	5.16	7	0.74		
Lack of fit	0.91	3	0.3	0.28	0.8355
Pure error	4.26	4	1.06		
Cor total	726.09	16			

Notes: ** extremely significant at $p<0.01$; * significant at $0.01<p<0.05$; the remaining are not significant at $p>0.05$; *df* means degree of freedom.

It can be known from the analysis results of Table 10 that the *p*-

value of the response surface model for the maximum tension Y_1 is <0.0001, which is less than 0.01, indicating that the finally obtained significance meets the requirements. The value of lack of fit is 0.8355, which is more than 0.005, indicating that the fitness of the model is relatively high and meets the requirements. The determination factor R of the model is 0.99. The data show that the fitness of the model is relatively high and the reliability of the response surface analysis results is relatively high. Hence, the model can predict and analyze the changes in the *Gentian* stem removal performance.

The regression terms X_1, X_3, X_1X_3, and X_2X_3 are extremely significant, while X_2 and X_1X_2 are significant. The significant factors affecting Y_1 in descending order are X_3, X_1, and X_2. In the interaction of factors, X_1X_3 and X_2X_3 had an extremely significant impact on Y_1.

Based on the data obtained in the experiment and on multiple regression fitting analysis by Design-Expert software, the mathematical regression model of the three independent variables, namely, the maximum tensile force Y_1 of the roller speed X_1, the spacing between stem-pulling rollers X_2, and the height of roller clamping position X_3, is established as follows:

$$Y_1 = 12.83 - 1.78X_1 - 0.97X_2 - 3.02X_3 + 1.50X_1X_2 + 3.22X_1X_3 + 2.11X_2X_3 + 7.4X_1^2 + 4.92X_2^2 + 6.15X_3^2 \quad (12)$$

A certain factor is fixed at the intermediate level to analyze the interactive effects of the other two factors on evaluation indices. Through plotting the response surface and contour plots, the three influencing factors on evaluation indices, namely, rollers speed, spacing between stem-pulling rollers, and the height of rollers clamping position, are analyzed, as shown in Figure 10. It can be seen from Figure 10 that the three factors affecting the maximum pulling force in the stem-removal rollers speed of about 190 r/min, stem-removal rollers spacing of about 2.75 mm, stem-removal rollers roll height of 240 mm when the maximum pulling force is the smallest. Too large or too small of a value for each of these three factors will make the maximum pulling force larger.

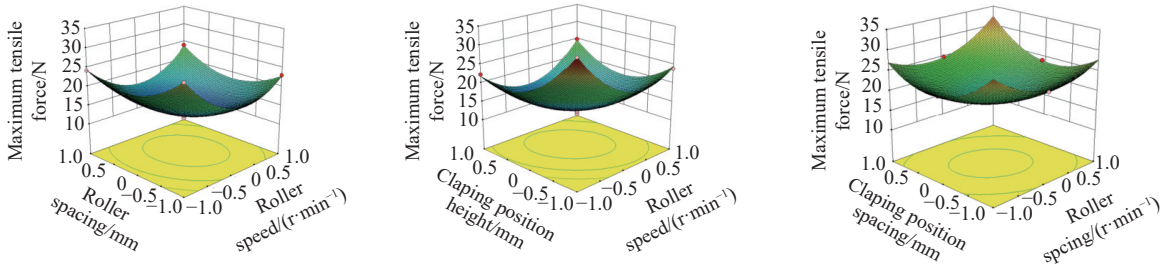

a. The interaction between the roller speed and the roller spacing on the maximum tensile force

b. The interaction between the roller speed and the clamping position height of the rolleron the maximum tensile force

c. The interaction between the roller spacing and the clamping position height of the rolleron the maximum tensile force

Figure 10 Response surface for the effect of each factor on maximum tensile force

The significance of the regression coefficients was tested for Y_2. The analysis results are listed in Table 11.

Table 11 Analysis of variance Y_2 regression model

Source	Sum of squares	*df*	Mean square	*F*-value	*p*-value
Model	427.47	9	47.5	91.07	<0.0001**
X_1	4.38	1	4.38	8.4	0.023*
X_2	96.26	1	96.26	184.56	<0.0001**
X_3	5.27	1	5.27	10.1	0.0155*
X_1X_2	6.71	1	6.71	12.86	0.0089**
X_1X_3	5.43	1	5.43	10.41	0.0145*
X_2X_3	4.6	1	4.6	8.82	0.0208*
X_1^2	135.73	1	135.73	260.25	<0.0001**
X_2^2	35.42	1	35.42	67.91	<0.0001**
X_3^2	104.22	1	104.22	199.84	<0.0001**
Residual	3.65	7	0.52		
Lack of Fit	1.81	3	0.6	1.31	0.3871
Pure Error	1.84	4	0.46		
Cor Total	431.12	16			

Notes: ** extremely significant at $p<0.01$; * significant at $0.01<p<0.05$; the remaining are not significant at $p>0.05$; *df* means degree of freedom.

It can be known from the analysis results of Table 11 that the *p*-value of the response surface model for the net removal rate Y_2 is <0.0001, which is less than 0.01, indicating that the finally obtained significance meets the requirements. The value of lack of fit is 0.3871, which is more than 0.005, indicating that the fitness of the model is relatively high and meets the requirements. The determination factor R of the model is 0.99. The data show that the fitness of the model is relatively high and the reliability of the response surface analysis results is relatively high. Hence, the model can predict and analyze the changes in the *Gentian* stems removal performance.

The regression terms X_2, X_1, and X_2 are extremely significant, while X_1, X_3, X_1X_3, and X_2X_3 are significant. The significant factors affecting Y_2 are in a descending order of X_2, X_3, and X_1. For interaction factors, X_1X_2 had an extremely significant impact on Y_1.

Based on the data obtained in the experiment and on multiple regression fitting analysis by Design-Expert software, the mathematical regression model of the three independent variables, namely, the net removal rate Y_2 of the roller speed X_1, spacing between stem-pulling rollers X_2, and height of roller clamping position X_3, is established as follows:

$$Y_2 = 97.99 + 0.74X_1 + 3.47X_2 + 0.81X_3 + 1.29X_1X_2 + 1.16X_1X_3 + 1.07X_2X_3 - 5.68X_1^2 - 2.90X_2^2 - 4.98X_3^2 \quad (13)$$

A certain factor is fixed at the intermediate level to analyze the interactive effects of the other two factors on evaluation indices. Through plotting the response surface and contour plots, the three influencing factors on evaluation indices, namely,rollers speed, spacing between stem-pulling rollers, and height of rollers clamping position, are analyzed, as shown in Figure 11. From this figure it can be seen that the net removal rate increased with the increase of roll spacing, and the net removal rate was maximum when the rollers spacing was about 3.1 mm. The net removal rate was maximum when the rollers speed was 190 r/min and the clamping position height of the roller was 240 mm. Too large or too small of a roller spacing and roller clamping position height will cause the net removal rate to decrease.

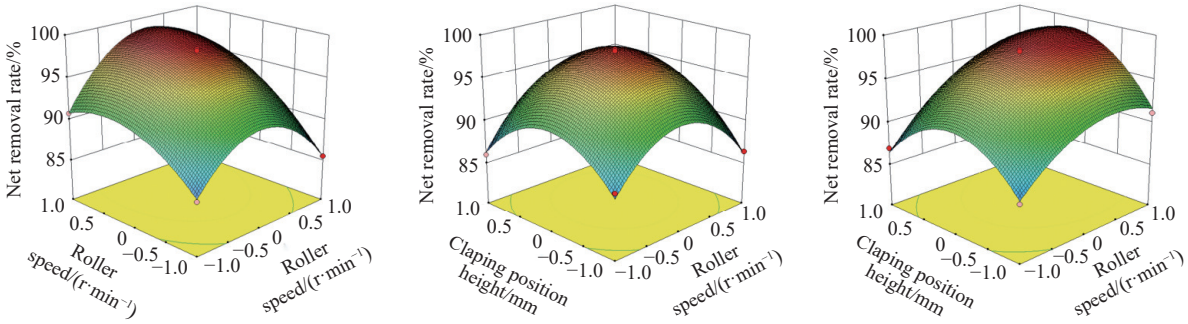

a. Interaction between the roller speed and roller spacing on net removal rate

b. Interaction between the roller speed and roller clamping position height on net removal rate

c. Interaction between the roller spacing and roller clamping position height on net removal rate

Figure 11 Response surface for the effect of each factor on the net removal rate

Combined with the analysis above, to optimize the *Gentian* stem removal performance, it is necessary to maximize the net removal rate and minimize the maximum tensile force. To seek the optimal parameter combination, it is necessary to conduct parameter optimization on multiple targets. The constraint conditions are listed below:

$$\begin{cases} 11\ \text{mm} \le Y_1 \le 35\ \text{mm} \\ \min Y_1 \\ \max Y_2 \\ 144\ \text{rpm} \le X_1 \le 239\ \text{rpm} \\ 2\ \text{mm} \le X_2 \le 3.5\ \text{mm} \\ 180\ \text{mm} \le X_3 \le 303\ \text{mm} \end{cases} \quad (14)$$

Design-Expert was used to optimize and solve each parameter. The optimal solutions are: roller speed 195.8 r/min, spacing between stem-pulling rollers 3.01 mm, height of roller clamping position 250.1 mm, maximum tensile force 12.85 N, and net removal rate 98.98%.

To verify the accuracy of the above model, a validation test was conducted with the same experimental method as before. Given the feasibility of experiment parameter setting, the optimized parameters were set as roller speed 195 r/min, spacing between stem-pulling rollers 3.0 mm, and height of roller clamping position 250 mm. In terms of experiment results, the maximum tensile force was measured as 13.88 N and the net removal rate was measured as 94.35%. The relative errors between the experiment values and optimized values were 8% and 5%, indicating that the results were relatively consistent. The research results can provide a reference for mechanism improvement of *Gentian* stem removal devices and operational parameter control.

5 Conclusions

(1) Based on the analysis of the mechanical properties of the *Gentian* stems and the force exerted on the *Gentian* stems during the removal process, the conditions for the complete removal of *Gentian* stems were determined. The tensile force exerted by the stem-pulling rollers on the *Gentian* stems should be less than the tensile force of the *Gentian* stems and greater than the maximum tensile force required for the *Gentian* stems to be removed at the stem bases. The tensile force exerted by the stem-pulling rollers should be applied to the bottom or middle of the stem where it is less broken.

(2) Through observation and analysis of the microstructure of the tree frog toe pad, it was found that the bionic surface composed of hexagonal prismatic units effectively improves the friction and adhesion of the working parts, and the flexible bionic surface achieves a certain effect of preventing the breakage of the *Gentian* stems. The bionic surface modeled on the microstructure of the tree frog toe pad effectively improves the friction performance of the rollers, protects the *Gentian* stems from breaking outside the stem base during the extraction process, and improves the net removal rate.

(3) The contact model between the *Gentian* stems and the bionic flexible stem-pulling rollers was constructed using EDEM discrete element simulation. The optimal combination of structural parameters of the bionic flexible surface was obtained through simulation tests. The results showed that when the diameter of the hexagonal unit was 5.67 mm, the spacing of adjacent hexagonal prisms was 2.62 mm, and the height of the hexagonal prism was 3.21 mm, the tensile force exerted by the stem-pulling rollers on the *Gentian* stems was the largest, and the pressure on the stems was the smallest.

(4) By building a bionic flexible stem-pulling roller test rig, the ternary quadratic combination test was designed with roller speed, roller spacing, and roller clamping position height as factors, and the tensile force and net removal rate of *Gentian* stems as indices. The test found the optimal parameter combination. The results showed that when roller speed was 195 r/min, roller spacing was 3.0 mm, and roller clamping position height was 250 mm, the tensile force required for *Gentian* stems to be removed completely was reduced to 13.88 N, and the net removal rate was increased to 94.35%.

Using the tree frog toe pad as a bionic prototype, preparing a bionic surface on the stem-pulling rollers can improve their working performance and boost the effectiveness of *Gentian* stem removal. This study should provide a reference for the development and optimization of *Gentian* stem harvesting.

Acknowledgements

The authors are grateful for the support of the Basic Scientific Research Program of the Education Department of Liaoning Province (Grant No. LJKMZ20220998) and the National Natural Science Foundation of China (Grant No. 52275264).

[References]

[1] Chang-Liao W L, Chien C F, Lin L C, Tsai T H. Isolation of gentiopicroside from Gentianae Radix and its pharmacokinetics on liver ischemia/reperfusion rats. J. Ethnopharm, 2012; 141: 668–673.

[2] Lian L H, Wu Y L, Wan Y, Li X, Xie W X, Nan J X. Anti-apoptotic activity of gentiopicroside in D-galactosamine/lipopolysaccharide-induced murine fulminant hepatic failure. Chemico-Biological Interactions, 2010;

188(1): 127–133.

[3] The State Pharmacopoeia Committee of China. The Pharmacopoeia of the People's Republic of China. Chemical Industry Press, Beijing, 2015; Part 1, 96p. (in Chinese)

[4] Kim J A, Son N S, Son J K, Jahng Y, Chang H W, Jang T S, et al. Two new secoiridoid glycosides from the rhizomes of Gentiana scabra Bunge. Arch. Pharm. Res., 2009; 32: 863–867.

[5] Sun J B, Li X Q, Wang X Y. Optimised design and analysis of potato harvesting machines. Journal of Agricultural Mechanization Research, 2017; 39(7): 83–88. (in Chinese)

[6] Zhang J, Wang J, Du D D. Design and testing of self-propelled tracked single-row cabbage harvester. Transactions of the CSAM, 2022; 53(12): 134–146. (in Chinese)

[7] Ji X, Du X W, Wang S G. Design and testing of a rootstock separator for carrot harvesters. Transactions of the CSAM, 2016; 47(3): 82–89. (in Chinese)

[8] Yu Z Y, Hu Z C, Wang H O. Optimisation and testing of the parameters of the garlic seedling separation mechanism. Transactions of the CSAE, 2015; 31(1): 40–46. (in Chinese)

[9] Wang J Y, Dong S P, Lv H Z. Development of cotton straw harvesting technology at home and abroad. 2008 Annual Academic Conference of the CSAM, Jinan, Shandong, China. 2008, 09.

[10] Zhang J X, Zhou H M, Cai J L. Design and testing of a cross shaft-to-roller straw lifting device. Transactions of the CSAE, 2021; 37(7): 43–52. (in Chinese)

[11] Zhang F, Wang W, Zhang G Y, Wang J, Qiu Z M, Mao P J. Gait analysis of goat at different slopes and study on biomimetic walking mechanism. Int J Agric & Biol Eng, 2016; 9(3): 40–47.

[12] Fu J, Qian Z H, Ren L Q. Morphologic effects of filiform papilla root on the lingual mechanical functions of Chinese yellow cattle. International Journal of Morphology, 2016; 34(1): 63–77.

[13] Kou T X. Key technology research on onion harvesting machine clamping and conveying device. Master Thesis. Qingdao University of Technology, 2019. (in Chinese)

[14] Ge Y, Zhang L X, Gu J W. Optimisation and testing of parameters for a roller-type saffron harvesting unit. Transactions of the CSAE, 2015; 31(21): 35–42. (in Chinese)

[15] Chirende B, Li J. Review on application of biomimetics in the design of agricultural implements. Biotechnology and Molecular Biology Reviews, 2009; 4(2): 42–48.

[16] Liu X M, Zhao DC, Chen L. Biomimetic tribology development status and application prospects. Chinese Journal of Construction Machinery, 2019; 17(2): 95–101. (in Chinese)

[17] Zhang Z X. Study of the frictional characteristics of face woven flexible friction pairs. Master Thesis. Shandong University of Science and Technology. Qingdao, Shandong Province, 2020. (in Chinese)

[18] Fu J, Zhang Y C, Chen Z. Design and testing of a bionic threshing tooth shape based on the filiform papillae structure of the yellow cow tongue. Transactions of the CSAM, 2019; 50(7): 167–176. (in Chinese)

[19] Wang C. Optimisation of the design of a bionic drum scraping and pulling banana stalk fibre extractor. Master Thesis. Hainan University. 2017. (in Chinese)

[20] Thirunavukkarasu N, Peng S Q, Gunasekaran H B, Yang Z, Wu L X, Weng Z X. Responsive friction modulation of 3D printed elastomeric bioinspired structures. Tribology International, 2022; 175: 107823.

[21] Zhang L W, Chen W H, Wang Y. Study of bionic surgical gripping surfaces based on wet adhesion of tree frog pedipalps. Journal of Mechanical Engineering, 2018; 54(17): 14–20. (in Chinese)

[22] Zhang L W, Chen W H, Zhang P F. Boundary friction study of a bionic hexagonal surface based on tree frog paws. Chinese Science Bulletin, 2016; 61(23): 2596–2604. (in Chinese)

[23] Chen X. Design and experimental study of a bionic structure to improve the tribological properties of rubber surfaces. Master Thesis. Jilin University, 2008. (in Chinese)

[24] Fu H, Wang C R, Jin C. Modelling methods for maturing wheat plants. Journal of Northeast Normal University (Natural Science Edition), 2017; 49(2): 64–68.

[25] Shi J R, Dai F, Zhao W Y. Experimental validation of discrete element flexibility modelling and contact parameters for caraway stems. Transactions of the CSAM, 2022; 53(10): 146–155.

[26] Xu Y F, Zhang X L, Wu S, Chen C, Wang J Z, Yuan S Q, et al. Numerical simulation of particle motion at cucumber straw grinding process based on EDEM. Int J Agric & Biol Eng, 2020; 13(6): 227–235.

[27] Guo Q, Zhang X L, Xu Y F. EDEM-based simulation and experimental study of the cutting performance of tomato straw. Journal of Drainage and Irrigation Machinery Engineering, 2018; 36(10): 1017–102.